The transport properties of $La_{0.8}Zr_{0.2}MnO_3$ film

2006 J. Phys.: Condens. Matter 18 741

(http://iopscience.iop.org/0953-8984/18/2/027)

INSTITUTE OF PHYSICS PUBLISHING JOURNAL OF PHYSICS: CONDENSED MATTER

J. Phys.: Condens. Matter **18** (2006) 741–750 doi:10.1088/0953-8984/18/2/027

The transport properties of $La_{0.8}Zr_{0.2}MnO_3$ film

D J Wang, Y W Xie, B G Shen and J R Sun

State Key Laboratory of Magnetism, Institute of Physics and Center for Condensed Matter Physics, Chinese Academy of Sciences, Beijing 100080, People's Republic of China

Received 6 September 2005, in final form 28 November 2005
Published 16 December 2005
Online at stacks.iop.org/JPhysCM/18/741

Abstract

The transport properties of the tetravalent ion-doped $La_{0.8}Zr_{0.2}MnO_3$ (LZMO) film, with strong magnetic–resistive correlation, have been studied. Vacuum annealing was adopted to modify the valence of Mn of the film. During the vacuum annealing process, the resistivity of the film increased overall and the metal–semiconductor transition shifted to lower temperature and finally vanished. The Hall effect studies revealed that the charge carriers were hole-like and the density of the carriers decreased with the oxygen escaping from the film. The x-ray photoelectron spectroscopy showed that the Mn ions in the film were driven from a mixture of Mn^{3+} and Mn^{4+} to that of Mn^{2+} and Mn^{3+}. When the Mn^{3+} and Mn^{2+} ions were dominant in the film, no resistive–magnetic correlation was observed. These results indicated that the magnetic–resistive correlation in the LZMO film was attributable to the interaction between Mn^{3+} and Mn^{4+} ions.

1. Introduction

The colossal magnetoresistance (CMR) effects in the manganite perovskite oxides $La_{1-x}M_xMnO_3$, where the M is a divalent ion such as Ca^{2+}, Sr^{2+}, Ba^{2+} or Pb^{2+}, have attracted worldwide attention [1]. The CMR effects can be explained by the double-exchange (DE) model qualitatively. In the DE scenario, the electron hopping between the Mn^{3+} and Mn^{4+} ions, with the help of intermediate oxygen, can produce a magnetic coupling among the ions [2, 3]. The presence of Mn ions with different valences is essential to DE. $LaMnO_3$ is an antiferromagnetic (AFM) semiconductor at low temperature because of the absence of Mn^{4+} ions [4]. Without DE, the superexchange between Mn^{3+} ions is dominant, and the activation-type conduction prevails due to the full occupation of the e_{g1} band and the complete emptiness of the e_{g2} band. Mn^{3+} ions can be oxidized into Mn^{4+} ions by replacing some of the La^{3+} ions with divalent ions, equivalently to doping holes into the e_{g1} band. On the other hand, if substituting some of the La^{3+} ions by tetravalent ions, Mn^{3+} ions will be deoxidized into Mn^{2+} ions, which is equivalent to introducing electrons into the e_{g2} band. Effects of tetravalent ion doping, including Ce^{4+}, Zr^{4+}, Sn^{4+} and Te^{4+}, have been studied extensively [5–13]. Mandal and Das [8] reported the Ce-doped $LaMnO_3$, and observed the paramagnetic–ferromagnetic (FM–PM)

transition and metal–semiconductor transition (MST), which were similar behaviours to the hole-doped manganites. Furthermore, the Ce-doped films were studied by photoemission/x-ray absorption spectroscopy and Hall effect to ascertain the electron-doped nature [9–11]. It seems, at a first glance, that all the data obtained were consistent with each other and could be accommodated into a frame based on electron-doping. To explain the strong magnetic–resistive correlation in the electron-doped manganites, the presence of DE between Mn^{2+} and Mn^{3+} has been proposed [8]. Recently, however, some groups have researched the $La_{0.7}Ce_{0.3}MnO_3$ film and found that the film was hole doped, not electron doped [12–14]. All these indicate that the character of the charge carriers in Ce doped manganites is under debate. To clarify the debate, it is necessary to further study other tetravalent ion-doping manganites. In fact, Hall effect measurement is a simple and effective means to distinguish the character of the charge carriers. In this paper, we report on the transport properties of a $La_{0.8}Zr_{0.2}MnO_3$ (LZMO) film, and find that the resistive–magnetic correlation is attributable to the interaction of Mn^{3+} and Mn^{4+} ions, not that of the Mn^{2+} and Mn^{3+} ions.

2. Experiment

The bulk target was prepared by solid-state reaction methods. La_2O_3, $MnCO_3$ and ZrO_2 powder with the La:Zr:Mn ratio of 0.8:0.2:1 were mixed in a mill for 1 h. The mixture was calcined in air at 950 °C for 16 h, followed by 1200 °C for 24 h with an intermediate grinding. The product was then pressed into a target after a ball milling of 2 h, and calcined in air at 1350 °C for 48 h.

The LZMO film of the thickness of ∼120 nm was grown on the (001) $LaAlO_3$ (LAO) single crystal substrate, using the pulsed laser ablation technique described elsewhere [15]. The temperature of the substrate was kept at 700 °C and the oxygen pressure was 80 Pa during the deposition. A post-annealing of the film at 700 °C for 30 min in air was performed to improve the crystallization of the film (called as-prepared sample hereafter).

The crystal structure of the film was characterized by the x-ray diffraction (XRD) measurement. The electrical resistivity was measured by a four-probe method, and the magnetic properties were studied by a superconducting quantum interference device (SQUID) magnetometer. X-ray photoelectron spectroscopy (XPS) was performed to analyse the valence of the Mn ions.

3. Results and discussion

Figure 1(a) shows the XRD pattern of the LZMO target. It is obvious that besides the peaks of the ABO_3 phase, the peaks of ZrO_2 appear, indicating that it is difficult for the Zr to be doped into manganites for the target. Figure 1(b) shows the XRD pattern of the LZMO film: only the reflection from the (00*l*) peaks of the LZMO film and the LAO substrate, no other peaks are detectable, demonstrating that the film was of single phase and *c*-axis orientated. The energy dispersive x-ray spectrometry (EDX) analysis gave a La:Zr:Mn ratio of 0.77:0.221:1, agreeing well with the target.

The temperature dependence of resistivity and magnetization for the as-prepared sample is shown in figure 2. The film is metallic below peak temperature ($T_p \sim 260$ K) and semiconductive above T_p. The simultaneous occurrence of MST and magnetic transition indicates a strong correlation between these two processes. In order to change the valence of Mn, the film was heated in a vacuum of $\sim 10^{-4}$ Pa to a predetermined temperature between 200 and 500 °C at a rate of ∼100 °C h^{-1}, then cooled to room temperature. Lower temperatures

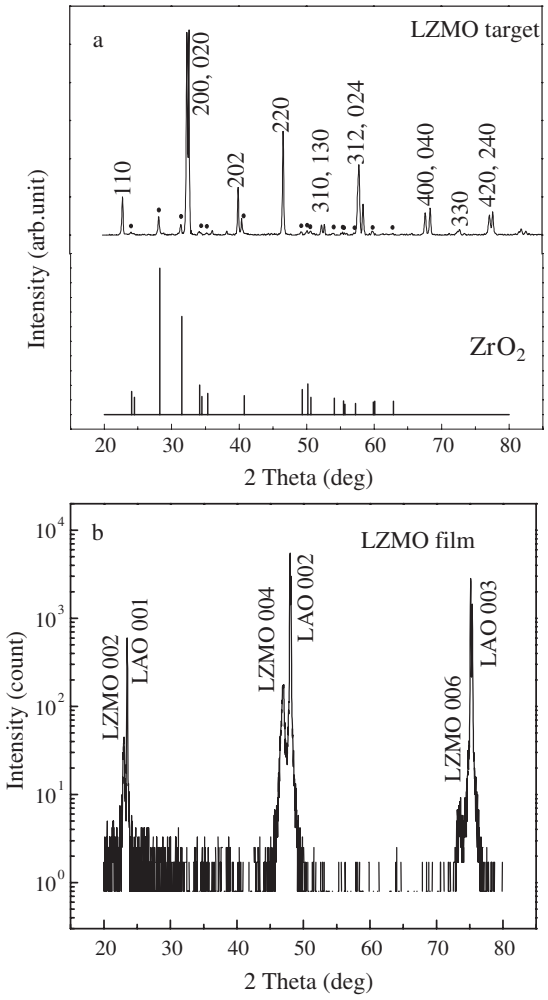

Figure 1. The XRD pattern of the LZMO. (a) The LZMO bulk target; (b) the LZMO film.

were used first to control the release of oxygen, then higher temperatures for a further oxygen depletion. After every annealing, the resistivity was measured as a function of temperature, as shown in figure 3. Vacuum annealing caused a gradual low-temperature shift of the MST, accompanying a considerable resistivity increase. The MST shifted from 260 K to ∼150 K, then vanished and never reappeared.

Effects of oxygen content on the crystal structure of the LZMO film have been studied by XRD. The change of the (004) peak of LZMO film after selected vacuum annealing is shown in figure 4(a). The peak moves to a lower angle, indicating an expansion of the out-of-plane lattice. The lattice expansion is produced by the deoxygenation of the Mn ions due to the release of oxygen. The MST temperature decreases linearly with the increase of the out-of-plane lattice constant from 260 to ∼150 K, then it vanishes for further oxygen release (figure 4(b)). The results are similar to that observed in the hole-doped $La_{0.67}Ca_{0.33}MnO_3$ (LCMO) film [16], which means that the MSTs of LZMO and LCMO films have a similar dependence on the oxygen content.

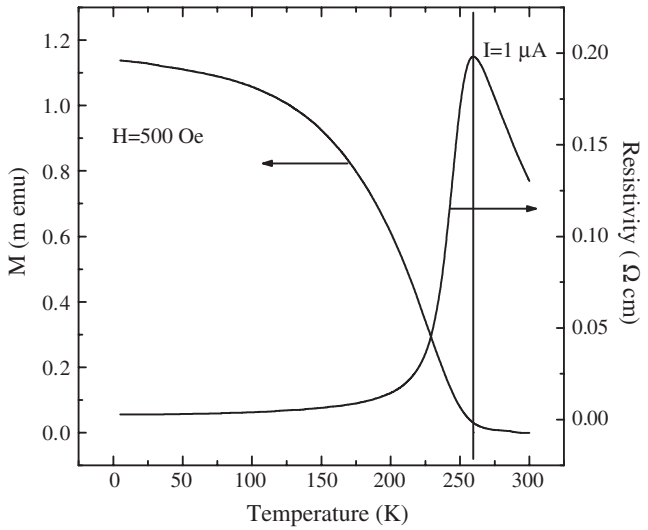

Figure 2. Temperature dependence of resistivity and magnetization of the as-prepared LZMO film. The thin line marks the simultaneous occurrence of resistive and magnetic transitions.

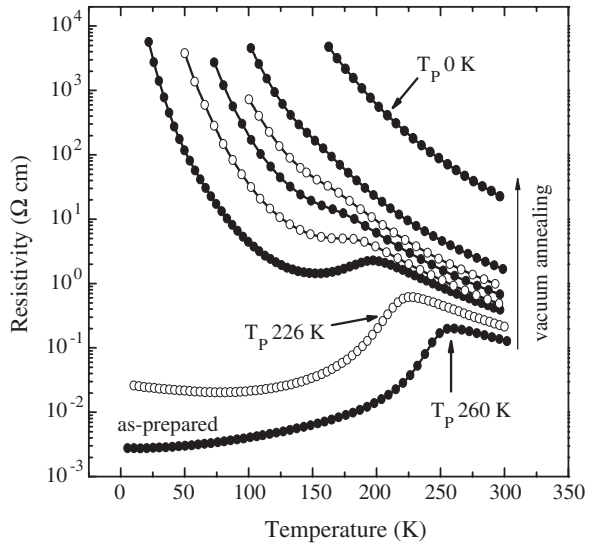

Figure 3. Temperature dependence of resistivity against vacuum annealing.

The resistivity obeys the following relation:

$$\rho(T) \propto T\rho_0 \exp(E_a/k_B T)$$

for a small polaron conduction [17], where ρ is the resistivity, E_a the activation energy and k_B the Boltzmann constant, respectively. This gives a satisfactory description for the LZMO film, as seen in figure 5(a). $\ln(\rho(T)/T)$ is linear with $1/T$ above T_p, and the activation energy E_a can be calculated from the slope. The activation energy increases with the expansion of the lattice (figure 5(b)), and the relation between E_a and the lattice constant can be fitted by a straight line. The activation energy of LCMO [16] was also given in contrast with that

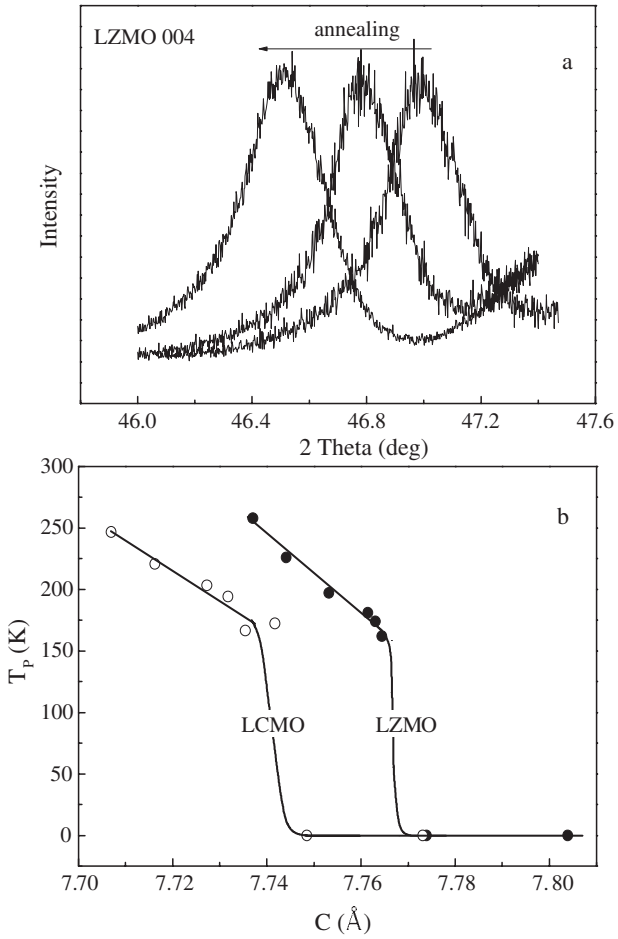

Figure 4. (a) The change of the (004) XRD peak of LZMO film after vacuum annealing. (b) The out-of-plane lattice constant dependence of the MST temperature; the data of the LCMO film are cited from [14].

of LZMO. It is interesting that the activation energies of LCMO and LZMO have the same relation to lattice constant, and also the same the activation energy, which indicates that the LZMO film and the LCMO film have similar relations between activation energy and oxygen content.

According to the proposal [8] that the DE between Mn^{2+} and Mn^{3+} determines the magnetic and transport properties of tetravalent ion doped manganites, the vacuum annealing will bring an increase of Mn^{2+} content, thus the interaction between the Mn^{2+} and Mn^{3+} will be strengthened. This actually leads to a decrease in resistivity and an increase in MST temperature. Obviously, it is a complete contradiction to the experimental results, implying that the assumed interaction between Mn^{2+} and Mn^{3+} ions may be incorrect. As an alternative, considering that the transport behaviours of the LZMO film are similar to the LCMO film, the strong magnetic–resistive interplay in the as-prepared sample may be attributed to the interaction between Mn^{3+} and Mn^{4+} ions. For the vacuum-annealed sample, the releasing of the oxygen leads to a decrease of the content of Mn^{4+} ions, which weakens the DE between

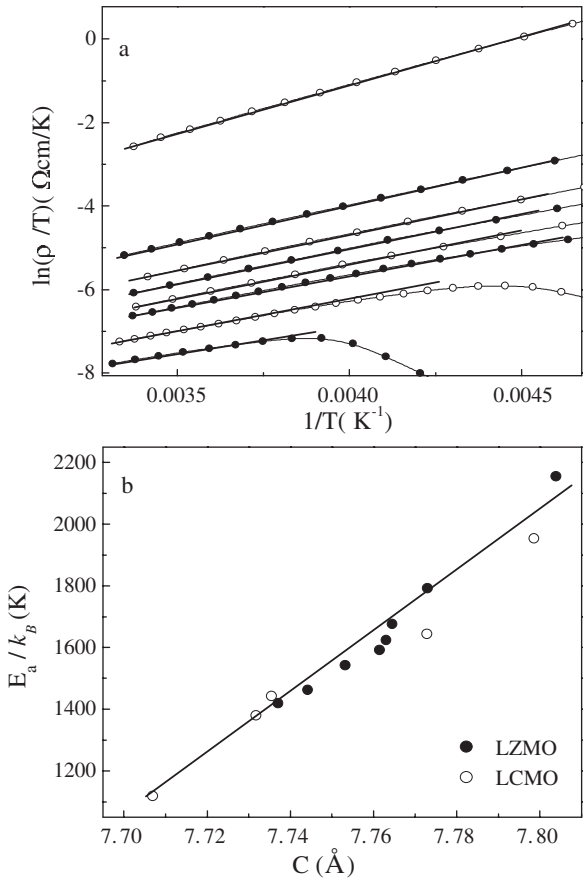

Figure 5. (a) $1/T$ dependence of $\ln(\rho(T)/T)$ of the LZMO film. (b) The relation between activation energy and the lattice constant of the LZMO film and LCMO film [14]. The solid line is a guide for the eye.

the Mn^{3+} and Mn^{4+} ions; consequently, the resistivity increases and the MST temperature decreases.

The Hall effects have been studied to distinguish the character of the charge carriers in the LZMO film. The film was patterned by the conventional lithographic method into a four-terminal Hall geometry. The Hall resistivity was measured on a commercial physical property measurement system (PPMS-14, Quantum Design). The experiment was performed in the temperature range from 25 to 275 K and the magnetic field (H) range from 0 to 10 T. An alternating current mode was used to eliminate undesired effects. Two Hall voltages were measured by rotating the sample by 180° around the applied current in a fixed field to remove the offset voltage due to the asymmetric Hall terminals or subsisting magnetoresistance.

The Hall resistivity (ρ_{xy}) against magnetic field for the as-prepared sample is shown in figure 6. It is clear that ρ_{xy} can be classified into two well-defined parts: the sharp drop in the low field range and the linear increase with applied field for higher fields. The former is called the anomalous Hall effect, due to the rotation of magnetic domains, while the latter is the normal one. This is a typical feature of a ferromagnet, and a simple description [18]

$$\rho_{xy} = R_S \mu_0 M + R_H \mu_0 H$$

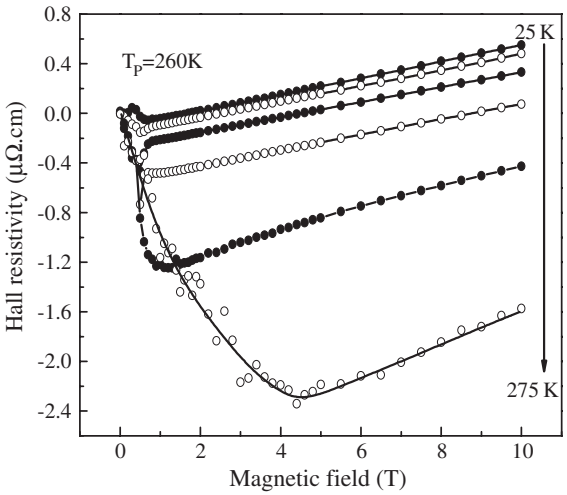

Figure 6. Magnetic field dependence of the Hall resistivity of the as-prepared LZMO film ($T_p = 260$ K) measured at various temperatures.

has been given if the demagnetization factor is set to unity, where R_S and R_H are the anomalous and normal Hall coefficients, respectively, μ_0 the vacuum permeability, and M the magnetization. The increase of temperature causes an inclining of the linear part of the ρ_{xy}–$\mu_0 H$ curve in the meantime enhancing the anomalous Hall effect, especially near the Curie temperature. It is interesting to note that the ρ_{xy}–$\mu_0 H$ slope for the linear part of this curve is positive. This reveals the hole-like character of the charge carriers; in other words, the substitution of Zr does not produce electron doping in the present case. We further studied the influence of vacuum annealing on the Hall effect to trace the variation of carrier type and density. It is found that the general features of the relation between ρ_{xy} and $\mu_0 H$ remain unaffected except for a change in the values of anomalous and normal Hall resistivity. The Hall effect stays hole-like down to $T_p = 226$ K, below which ($T_p < 226$ K) the large offset voltage and magnetoresistance disturb a reliable determination of ρ_{xy}.

The effective carrier number calculated from R_H using $R_H = 1/qn$ is shown in figure 7 as a function of temperature. It is ∼0.55 holes/Mn site at $T = 25$ K for the as-prepared sample. With the increase of temperature, the carrier number exhibits a slight increase and saturates at ∼0.6 holes/Mn site above 135 K. This value is smaller than that observed in $La_{0.7}Ca_{0.3}MnO_3$ (∼2 holes/Mn site), but comparable to $La_{0.7}Sr_{0.3}MnO_3$ (∼1 holes/Mn site) [19]. A steep drop of the carrier density appears as the temperature approaches T_p, which has been observed in other manganites [20, 21] and attributed to the change of conduction mechanism around T_p [22]. Vacuum annealing leads to a decrease of n. The Hall effect results are consistent with the previous vacuum annealing data.

The x-ray photoelectron spectroscopy (XPS) was also performed on the film to verify the valence of the Mn (figure 8). For the as-prepared sample, the Mn $2p_{3/2}$ peak is located at 642.0 eV, which is between the values of peaks of Mn^{4+} (642.2 eV) and Mn^{3+} (641.8 eV) (the binding energy of Mn $2p_{3/2}$ of Mn^{2+} is 640.6 eV [6]). The XPS spectrum of Mn in $La_{0.7}Ca_{0.3}MnO_3$ was also given to be compared with that of LZMO film. The coincidence of the Mn 2p spectrum of the as-prepared sample with that of $La_{0.7}Ca_{0.3}MnO_3$ indicates a similar Mn ion valence in the two manganites. Those results imply that the Mn^{3+} and Mn^{4+} ions dominate in the as-prepared film and the sample is hole doped. Obviously, the valence of

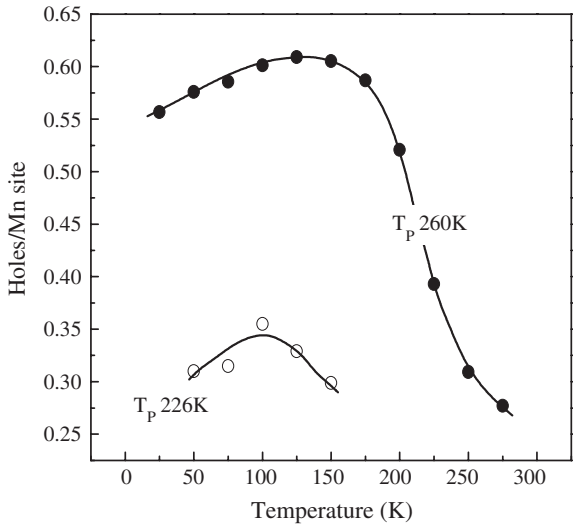

Figure 7. Carrier density as a function of temperature. Solid lines are guides for the eye.

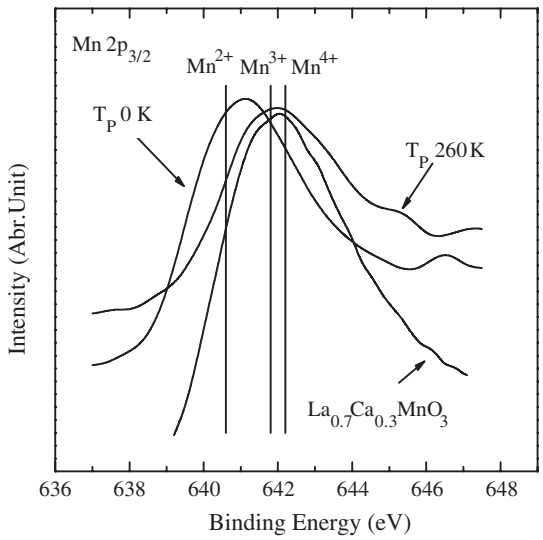

Figure 8. Mn 2p XPS spectra of as-prepared sample and the last vacuum-annealed sample (T_p 0 K). The Mn 2p XPS spectrum of $La_{0.7}Ca_{0.3}MnO_3$ is given in contrast with that of LZMO. Peak positions for Mn^{2+}, Mn^{3+} and Mn^{4+} are marked by thin lines.

the Mn ions will decrease when the oxygen escapes from the film. The oxygen release even drives the Mn^{3+} and Mn^{4+} ions into Mn^{2+}, which is confirmed by the XPS spectrum of the last vacuum-annealed sample (T_p 0 K). The Mn $2p_{3/2}$ peak is located at 640.9 eV, between the peaks of Mn^{2+} and Mn^{3+}, indicating that the Mn^{2+} and Mn^{3+} ions dominate in the sample and the film is truly electron doped, but in this electron-doped film there is no MST observed and the resistivity is extremely large, which is obviously different from the electron-doped manganites reported previously.

The reasons for the appearance of hole-like doping effects could be the presence of cation vacancies. There are two possibilities for introducing the cation vacancies. One is the composition distribution in the sample. The nanometre ZrO_2 domains may be formed in the LZMO, which could not be detected by x-ray diffraction, just like the Ce-doped manganites [12]. However, the structure and lattice constant of ZrO_2 are completely different from those of CeO_2, which means that it is difficult for ZrO_2 to grow epitaxially in the LZMO film, so the density of the nanometre ZrO_2 domain should be very low. The other possibility for the cation vacancies is excessive oxygen in the sample, which may always occur accompanying tetravalent ion doping due to the requirement for chemical equilibrium. As a consequence, the Mn ions mainly stay in the state of Mn^{3+} and Mn^{4+}. Mn^{2+} ions could also exist; however, their content may not be high. It is easy to show that to get a Mn^{4+}:Mn^{3+} ratio of 0.2:0.8 excessive oxygen content of $\sim$8% is enough, within the tolerance of manganite perovskites. In fact, it has been revealed that for the manganites Mn ions prefer to stay in the Mn^{3+} and Mn^{4+} mixed valence state, and in the case of Mn^{3+}:Mn^{4+} = 0.7:0.3 it is difficult to remove oxygen from or insert oxygen into the manganite lattice [23]. This explains why significant excessive oxygen always exists in the $LaMnO_3$ films prepared under the conditions for an ordinary hole-doped manganite film. With this in mind, excessive oxygen in LZMO is possible. The presence of cation vacancies can also be recognized from the resistive behaviour of LZMO. It is found that the residual resistivity of the as-prepared LZMO film is $\sim 2.7 \times 10^{-3}$ Ω cm, much larger than that of the LCMO film [14] ($\sim 4 \times 10^{-4}$ Ω cm) with a similar Curie temperature.

4. Conclusion

In summary, the transport properties of the $La_{0.8}Zr_{0.2}MnO_3$ film with strong magnetic–resistive correlation, which was believed to be an electron-doped manganite, have been studied. Releasing oxygen by annealing the film in vacuum drove the resistivity of the film to increase and the MST temperature to decrease. These were behaviours usually occurring in a hole-doped manganite. The hole-like character of the charge carrier was further confirmed by Hall effects and the XPS data. It is possible that the presence of cation vacancies counteracts the effect of Zr^{4+} ions, resulting in a hole-doping effect. When the average valence of Mn was less than 3+, i.e., the sample was truly electron doped, no magnetic–resistive correlation was observed. The results will be helpful to understand the CMR effect of the tetravalent cation-doped manganites.

Acknowledgments

This work has been supported by the National Natural Science Foundation of China and the State Key Project for Fundamental Research of China.

References

[1] For a review, see Rao C N R and Raveau B (ed) 1998 *Colossal Magnetoresistance, Charge Ordering, and Related Properties of Manganese Oxides* (Singapore: World Scientific)
Tokura Y (ed) 1999 *Colossal Magnetoresistance Oxides* (London: Gordon and Breach)
[2] Zener C 1951 *Phys. Rev.* **82** 403
[3] Anderson P W and Hasegawa H 1955 *Phys. Rev.* **100** 675
[4] Millis A J 1998 *Nature* **392** 147
[5] Roy S and Ali N 2001 *J. Appl. Phys.* **89** 7425
[6] Gao J, Dai S Y and Li T K 2003 *Phys. Rev.* B **67** 153403

[7] Tan G T, Dai S Y, Duan P, Zhou Y L, Lu H B and Chen Z H 2003 *J. Appl. Phys.* **93** 5480
Tan G T, Zhang X and Chen Z 2004 *J. Appl. Phys.* **95** 6322
[8] Mandal P and Das S 1997 *Phys. Rev.* B **56** 15073
[9] Mitra C, Raychaudhuri P, John J, Dhar S K, Nigam A K and Pinto R 2001 *J. Appl. Phys.* **89** 524
[10] Mitra C, Raychaudhuri P, Dörr K, Müller K-H, Schultz L, Oppeneer P M and Wirth S 2003 *Phys. Rev. Lett.* **90** 17202
[11] Han S W, Kang J-K, Kim K H, Lee J D, Kim J H, Wi S C, Mitra C, Raychaudhuri P, Wirth S, Kim K J, Kim B S, Jeong J I, Kwon S K and Min B I 2004 *Phys. Rev.* B **69** 104406
[12] Yanagida T, Kanki T, Vilquin B, Tanaka H and Kawai T 2004 *Phys. Rev.* B **70** 184437
[13] Yanagida T, Kanki T, Vilquin B, Tanaka H and Kawai T 2005 *J. Appl. Phys.* **97** 033905
[14] Chang W J, Tsai J Y, Jeng H-T, Lin J-Y, Zhang Kenneth Y-J, Liu H L, Lee J M, Chen J M, Wu K H, Uen T M, Gou Y S and Juang J Y 2005 *Preprint* cond-mat 0509391
[15] Sun J R, Xiong C M, Zhao T Y, Zhang S Y, Chen Y F and Shen B G 2004 *Appl. Phys. Lett.* **84** 1528
[16] Sun J R, Yeung C F, Zhao K, Zhou L Z, Leung C H, Wong H K and Shen B G 2000 *Appl. Phys. Lett.* **76** 1164
[17] Coey J M D, Viret M and Von Molnár S 1999 *Adv. Phys.* **48** 167
[18] Karplus R and Luttinger J M 1954 *Phys. Rev.* **55** 1154
[19] Lynda-Geller Y, Chun S H, Salamon M B, Goldbart P M, Han P D, Tomioka Y, Asamitsu A and Tokura Y 2001 *Phys. Rev.* B **63** 184426
[20] Wagner P, Gordon I, Vantomme A, Dierickx D, Van Beal M J, Moshchalkov V V and Bruynseraede Y 1998 *Europhys. Lett.* **41** 49
[21] Chun S H, Salamon M B and Han P D 1999 *Phys. Rev.* B **59** 11155
[22] Jaime M, Liu P, Chun S H, Salamon M B, Dorsey P and Rubinstein M 1999 *Phys. Rev.* B **60** 1028
[23] Ju H L, Gopalakrishnan J, Peng J L, Li Q, Xiong G C, Venkatesan T and Greene R L 1995 *Phys. Rev.* B **51** 6143